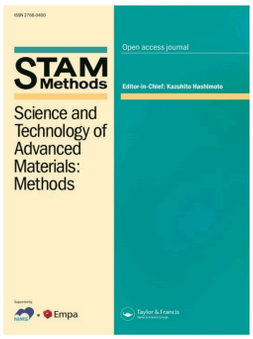

Science and Technology of Advanced Materials: Methods

ISSN: 2766-0400 (Online) Journal homepage: www.tandfonline.com/journals/tstm20

Creep data sheet for 9Cr-1Mo-V-Nb steel tubes, plates and pipe

Kazuhiro Kimura, Yasushi Taniuchi, Kaoru Sekido, Takehiro Nojima, Tomotaka Hatakeyama & Kota Sawada

To cite this article: Kazuhiro Kimura, Yasushi Taniuchi, Kaoru Sekido, Takehiro Nojima, Tomotaka Hatakeyama & Kota Sawada (2025) Creep data sheet for 9Cr-1Mo-V-Nb steel tubes, plates and pipe, Science and Technology of Advanced Materials: Methods, 5:1, 2588872, DOI: 10.1080/27660400.2025.2588872

To link to this article: https://doi.org/10.1080/27660400.2025.2588872

Published online: 02 Dec 2025.

SCIENCE AND TECHNOLOGY OF ADVANCED MATERIALS: METHODS
2025, VOL. 5, NO. 1, 2588872
https://doi.org/10.1080/27660400.2025.2588872

Creep data sheet for 9Cr-1Mo-V-Nb steel tubes, plates and pipe

Kazuhiro Kimura[a], Yasushi Taniuchi[b], Kaoru Sekido[b], Takehiro Nojima[b], Tomotaka Hatakeyama[a] and Kota Sawada[a]

[a]Research Center for Structural Materials, National Institute for Materials Science, Tsukuba, Japan; [b]Research Network and Facility Services Division, National Institute for Materials Science, Tsukuba, Japan

ABSTRACT

Creep data of 9Cr-1Mo-V-Nb steel tube, plate, and pipe steels (ASME SA-213/SA-213 M Grade T91 Type 1, SA-387/SA-387 M Grade 91 Type 1, and SA-335/SA-335 M Grade P91 Type 1) were obtained in the temperature range of 450°C to 725°C and the stress range of 30MPa to 450MPa. The short-term tensile properties of the steels were also evaluated over a range of temperatures from room temperature to 750°C. Creep rupture data were regression analysed using Larson-Miller and Orr-Sherby-Dorn parameter with and without region splitting analysis (RSA) method. The result of creep rupture data evaluation using Larson-Miller parameter by means of RSA method with third and second order polynomials for high- and low-stress regimes, respectively, was the most appropriate and accurate. Minimum creep rate data was also evaluated by the same manner as time to rupture. Temperature dependence of 0.2% proof stress, tensile strength, and creep rupture strength at 100, 1,000, 10,000, and 100,000 h for 9Cr-1Mo-V-Nb tube, plate, and pipe steels.

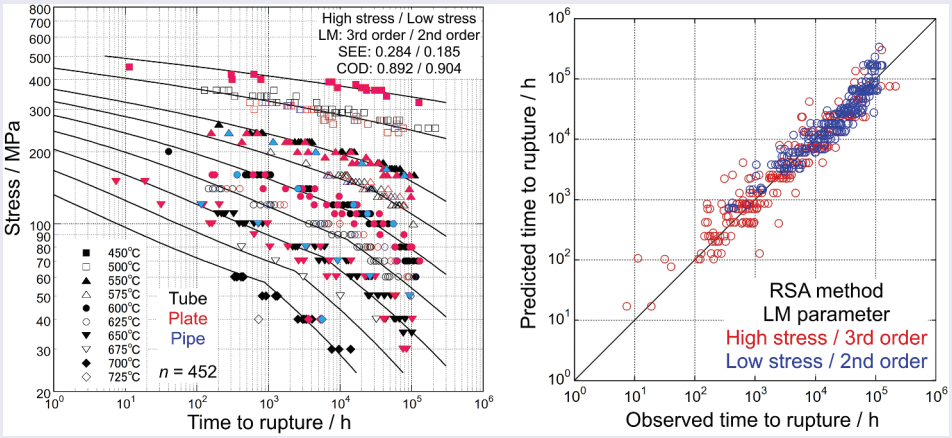

ARTICLE HISTORY
Received 4 June 2025
Revised 4 November 2025
Accepted 9 November 2025

KEYWORDS
Creep strength enhanced ferritic steel; Grade 91; creep rupture strength; 100,000 h; minimum creep rate; time-temperature parameter; region splitting analysis

IMPACT STATEMENT

This manuscript reports on results of creep data analysis on Grade 91 steels by means of Region Splitting Analysis method based on long-term creep test data obtained in NIMS.

1. Introduction

Creep strength enhanced ferritic (CSEF) steels represented by 9Cr-1Mo-V-Nb steels (ASTM/ASME Grade 91 Type 1) are strengthened by precipitation strengthening effect of $M_{23}C_6$ carbide and fine MX carbonitrides, solid solution strengthening of molybdenum and/or tungsten with a tempered martensitic microstructure [1]. Because of its improved creep strength, CSEF steels have been widely used for high temperature structural components in modern thermal power plants, and it has contributed to improve thermal efficiency. On the other hand, a risk of overestimation of long-term creep strength of CSEF steels due to microstructural change during creep exposure at the elevated temperatures which causes degradation of mechanical property has been pointed out [2–4]. Moreover, cases of damage occurring to CSEF steel components in operating power plants have been reported [5–8]; therefore, extensive research has been conducted to determine the cause of the degradation in creep strength of CSEF steels. Precipitation of Z-phase that is a complex nitride of chromium, vanadium and niobium has been reported as a candidate cause to reduce creep strength [3,9,10], as well as a precipitation of Laves

CONTACT Kazuhiro Kimura KIMURA.Kazuhiro@nims.go.jp Research Center for Structural Materials, National Institute for Materials Science, 1-2-1 Sengen, Tsukuba, Ibaraki 305-0047, Japan

phase [11,12]. Lowered nitrogen content in solid solution was considered as a cause of low strength and a ratio of nitrogen to aluminium (N/Al) was suggested as a useful indicator of creep strength [5–7]. It has been reported that nickel is a harmful element, since it promotes microstructural change and precipitation of Z-phase [13], existence of delta-ferrite phase and a remaining of solidification segregation are also harmful because those promote microstructural change during creep exposure [14,15]. In addition, inhomogeneous recovery preferentially taking place in the vicinity of prior austenite grain boundary was reported as a cause of large drop in creep strength in the long term [4,10].

Allowable stress at the elevated temperatures is determined based on the long-term creep strength of 100,000 h creep rupture strength and a stress causes minimum creep rate of 10^{-7} h^{-1} [16,17]; therefore, the review of allowable stress has been carried out based on the assessment of long-term creep strength [8,18,19], in parallel with the investigation into the cause of the decrease in creep strength. In the present study, tensile and creep strength properties were analysed, and a 100,000 h creep rupture strength was estimated for 9Cr-1Mo-V-Nb steel tubes, plates, and pipe.

2. Experimental procedures

2.1. Material

The materials examined were 9Cr-1Mo-V-Nb steel tubes, plates and pipe steels (ASME Grade T91 Type 1, Grade 91 Type 1, and Grade P91 Type1, respectively [20]). Details such as the type of melting, product form, processing, and thermal history are listed in Tables 1(a,b). Six commercial heats of tube, four commercial heats of plate and single commercial heat of pipe were sampled from several steel manufacturers for tensile and creep testing. In the NIMS Creep Data Sheet Project, several commercial heats are normally selected because the users of the material need to know the heat-to-heat variation of the creep strength to design components. Table 2 shows the chemical compositions of the 2(a) tubes, 2(b) plates, and 2(c) pipe steels. All the compositions were within the range of specifications of ASME Boiler and Pressure Vessel Code, Section II, Part-A [20].

2.2. Tensile and creep testing

Tensile testing was conducted at temperatures ranging from 24°C to 750°C in accordance with JIS G 0567–1998 [21]. The engineering (nominal) strain rate of the specimens was controlled to 5×10^{-5} s^{-1} up to about 1.0% proof stress and 1.25×10^{-3} s^{-1} beyond that.

Creep testing at 450°C to 725°C was performed in accordance with JIS Z 2271–1998 [22]. Creep strain – time data were obtained using single-type creep testing machines developed by the National Research Institute for Metals (NRIM), the former organization of NIMS. Solid cylindrical specimens with a gauge diameter of 6 mm for tube steels and 10 mm for plate and pipe steels as shown in Figure 1 were used.

2.3. Temperature measurement and control

The degree of temperature used in the tensile and creep testing was based upon the International Temperature Scale of 1990 [23]. The temperature was maintained to within ±3°C for temperature equal to or higher than 100°C but equal to or lower than 725°C.

2.4. Microstructure observation

For observation by an optical microscope, the creep-ruptured specimens were cut longitudinally parallel to

Table 1. Details of 9Cr-1Mo-V-Nb steel tubes, plates and pipe.

NIMS reference code	Type of Melting[b]	Size of ingot (kg)	Deoxidation process	Product form	Dimensions[c] (mm)	Processing and thermal history[d]	Austenite grain size number[e]	Rockwell hardness (HRC)	Non-metallic Inclusion[f] (%)
(a) Details of 9Cr-1Mo-V-Nb steel tubesa									
MGA	BEA	3,500	Al-Si-killed	Tube	50.8 OD	Hot extruded and cold drawn	10.1	16	*d* A = 0.00
					8.0 WT	1 045°C/10 min AC			*d* B = 0.00
					6 000 L	780°C/60 min AC			*d* C = 0.02
MGB	BEA	7,000	Al-killed	Tube	50.8 OD	Hot extruded and cold drawn	9.3	16	*d* A = 0.00
					7.3 WT	1 050°C/60 min AC			*d* B = 0.00
					6 000 L	760°C/60 min AC			*d* C = 0.05
MGC	BEA	C.C.[g]	Si-killed	Tube	50.8 OD	Hot extruded and cold drawn	10.2	18	*d* A = 0.00
					8.0 WT	1 050°C/10 min AC			*d* B = 0.02
					5 000 L	765°C/30 min AC			*d* C = 0.02
MGD	LDC	12,000	Al-Si-killed	Tube	50.8 OD	Hot extruded and cold drawn	10.2	18	*d* A = 0.00
					8.9 WT	1 050°C/10 min AC			*d* B = 0.00
					5 100 L	780°C/40 min AC			*d* C = 0.04
MGF	BEA	C.C.	Si-Al-killed	Tube	50.8 OD	Hot extruded	10.6	18	*d* A = 0.01
					8.7 WT	1 045°C/60 min AC			*d* B = 0.00
					5 000 L	780°C/60 min AC			*d* C = 0.05
MGG	TBBC	C.C.	VD[h]	Tube	50.8 OD	Hot extruded	10.7	18	*d* A = 0.01
					9.0 WT	1 050°C/15 min AC			*d* B = 0.02
					5 500 L	790°C/60 min AC			*d* C = 0.01

(*Continued*)

Table 1. (Continued).

NIMS reference code	Type of Melting[b]	Size of ingot (kg)	Deoxidation process	Product form	Dimensions[c] (mm)	Processing and thermal history[d]	Austenite grain size number[e]	Rockwell hardness (HRC)	Non-metallic Inclusion[f] (%)
(b) Details of 9Cr-1Mo-V-Nb steel plates and pipea									
MgA	BEA	13 500	Al-Si-killed	Plate	25 T 2 150 W 9 477 L	Hot rolled 1 050°C/10 min AC 770°C/60 min AC 740°C/8.4 h FC	10.4	13	*d* A = 0.00 *d* B = 0.00 *d* C = 0.02
MgB	BEA	13 500	Al-Si-killed	Plate	25 T 2 150 W 9 477 L	Hot rolled 1 050°C/10 min AC 770°C/60 min AC 740°C/60 min FC	10.4	14	*d* A = 0.00 *d* B = 0.00 *d* C = 0.02
MgC	LDC	20 000	Al-Si-killed	Plate	50 T 2 200 W 15 000 L	Hot rolled 1 060°C/90 min AC 760°C/60 min AC 730°C/8.4 h FC	9.3	17	*d* A = 0.00 *d* B = 0.02 *d* C = 0.01
MgD	LDC	26 000	Al-Si-killed	Plate	25 T 1 000 W 3 000 L	Hot rolled 1 050°C/30 min AC 780°C/30 min AC	8.8	16	*d* A = 0.00 *d* B = 0.01 *d* C = 0.05
MGQ	BEA	80 000	Si-Al-killed	Pipe	355 OD 35.7 WT 6 000 L	Hot rolled 1 060°C/60 min AC 780°C/60 min AC	8.8	15	*d* A = 0.00 *d* B = 0.01 *d* C = 0.04

[a]The tubes were sampled in 1990 (MGA, MGB and MGC), 2000 (MGD) and 2001 (MGF and MGG), the plates were sampled in1988 (MgA, MgB), 1991 (MgC) and 2002 (MgD), the pipe was sampled in 2002.
[b]BEA: basis electric arc furnace, LDC: LD converter, TBBC: top and bottom blown converter.
[c]OD: outside diameter, WT: wall thickness, L: length, T: thickness.
[d]AC: air cooling, FC: furnace cooling.
eJIS G 0551–2020, 'Steels – Micrographic determination of the apparent grain size'.
[f]JIS G 0555–2023, 'Microscopic testing method for the non-metallic inclusions in steel'.
[g]C.C.: Continuous Casting.
[h]VD: vacuum degassing.

Table 2. Chemical composition (product analysis) of 9Cr-1Mo-V-Nb steel (a) tubes, (b) plates and (c) pipe.

NIMS reference code	Chemical composition (mass percent)[a]													
	C	Si	Mn	P	S	Ni	Cr	Mo	V	Nb*	N	Al*	Ti*	Zr*
(a) Chemical composition (product analysis) of 9Cr-1Mo-V-Nb steel tubes.														
Requirement[b]	0.07 – 0.14	0.20 – 0.50	0.30 – 0.60	≤0.020	≤0.010	≤0.40	8.0 – 9.5	0.85 – 1.05	0.18 – 0.25	0.06 – 0.10	0.030 – 0.070	≤0.04[c] ≤0.02	–[c] ≤0.01	–[c] ≤0.01
MGA	0.10	0.38	0.40	0.015	0.001	0.12	8.53	0.96	0.21	0.076	0.050	0.014	< 0.001	< 0.001
MGB	0.09	0.34	0.45	0.015	0.001	0.20	8.51	0.90	0.205	0.076	0.042	0.016	0.001	< 0.001
MGC	0.09	0.29	0.35	0.009	0.002	0.28	8.70	0.90	0.22	0.072	0.044	0.001	< 0.001	< 0.001
MGD	0.10	0.29	0.41	0.010	0.001	0.10	8.41	0.90	0.185	0.07	0.048	0.016	0.001	< 0.001
MGF	0.11	0.25	0.42	0.013	0.001	0.06	8.41	0.91	0.20	0.08	0.053	0.001	0.006	< 0.001
MGG	0.10	0.38	0.37	0.018	0.002	0.12	8.60	0.95	0.190	0.08	0.0458	0.002	< 0.001	< 0.001
(b) Chemical composition (product analysis) of 9Cr-1Mo-V-Nb steel plates.														
Requirement[d]	0.06 – 0.15	0.18 – 0.56	0.25 – 0.66	≤0.025	≤0.012	≤0.43	7.90 – 9.60	0.80 – 1.10	0.16 – 0.27	0.05 – 0.11	0.025 – 0.080	≤0.05[e] ≤0.02	–[e] ≤0.01	–[e] ≤0.01
MgA	0.08	0.34	0.49	0.005	0.004	0.09	8.34	0.89	0.23	0.070	0.059	0.012	< 0.001	< 0.001
MgB	0.08	0.34	0.49	0.005	0.004	0.09	8.34	0.89	0.23	0.070	0.059	0.012	< 0.001	< 0.001
MgC	0.10	0.24	0.44	0.005	0.001	0.04	8.74	0.94	0.21	0.076	0.0582	0.014	< 0.001	< 0.001
MgD	0.11	0.29	0.45	0.008	0.001	0.08	8.44	0.99	0.21	0.09	0.050	0.023	0.001	< 0.001
(c) Chemical composition (product analysis) of 9Cr-1Mo-V-Nb steel pipe.														
Requirement[f]	0.08 – 0.12	0.20 – 0.50	0.30 – 0.60	≤0.020	≤0.010	≤0.40	8.00 – 9.50	0.85 – 1.05	0.18 – 0.25	0.06 – 0.10	0.030 – 0.070	≤0.04[c] ≤0.02	–[g] ≤0.01	–[g] ≤0.01
MGQ	0.11	0.24	0.43	0.014	0.002	0.08	8.31	0.92	0.19	0.07	0.046	0.001	0.005	< 0.001

[a]The chemical composition given above was reported by the steel manufacturers except for the elements marked with asterisk, for which the analysis was carried out at NRIM and NIMS.
[b]ASME SA-213/SA-213 M Grade T91 Type 1, Product analysis, 2023. SPECIFICATION FOR SEAMLESS FERRITIC AND AUSTENITIC ALLOY-STEEL BOILER, SUPERHEATER, AND HEAT EXCHANGER TUBES.
[c]ASME SA-213/SA-213 M Grade T91, Product analysis, 2007. SPECIFICATION FOR SEAMLESS FERRITIC AND AUSTENITIC ALLOY-STEEL BOILER, SUPERHEATER, AND HEAT EXCHANGER TUBES.
[d]ASME SA-387/SA-387 M Grade 91 Type 1, Product analysis, 2023. SPECIFICATION FOR PRESSURE VESSEL PLATES, ALLOY STEEL, CHROMIUM-MOLYBDENUM.
[e]ASME SA-387/SA-387 M Grade 91, Product analysis, 2007. SPECIFICATION FOR PRESSURE VESSEL PLATES, ALLOY STEEL, CHROMIUM-MOLYBDENUM.
[f]ASME SA-335/SA-335 M Grade P91 Type 1, Heat analysis, 2023. SPECIFICATION FOR SEAMLESS FERRITIC ALLOY-STEEL PIPE FOR HIGH-TEMPERATURE SERVICE.
[g]ASME SA-335/SA-335 M Grade P91, Heat analysis, 2007. SPECIFICATION FOR SEAMLESS FERRITIC ALLOY-STEEL PIPE FOR HIGH-TEMPERATURE SERVICE.

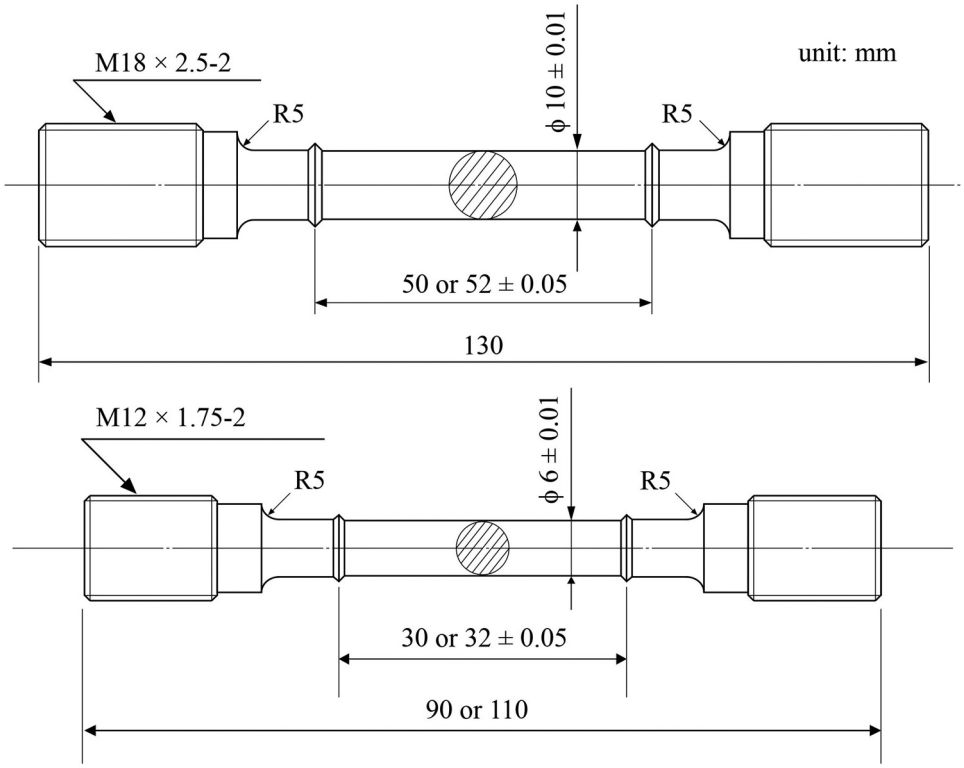

Figure 1. Specimens for tensile and creep tests.

the stress direction using a water-cooled fine cutter, then embedded in hard resin, and then polished with emery paper and buffing cloths with paste. The samples were etched with 4 g $C_6H_3O_7N_3$, 1 ml HCl, and 100 ml C_2H_5OH.

3. Analysis methods

3.1. Tensile data

Regression analysis of the tensile data was conducted using the following equation:

$$\log\left(S_y \text{ or } S_T\right) = a_0 + a_1 T + a_2 T^2 + \ldots + a_k T^k \quad (1)$$

where S_y = 0.2% proof stress (MPa),
S_T = tensile strength (MPa),
T = temperature (°C),
a_0, a_1, a_2, … a_k = regression coefficients estimated by the least square method, and k = degree of regression equation.

3.2. Creep rupture data

Regression analysis of the creep test data was performed using a regression equation of logarithmic stress with the time-temperature parameters (P) of Larson-Miller (LM) [24], and Orr-Sherby-Dorn (OSD) [25] as follows:

$$\mathrm{LM}P = (T + 273.15)(C + logt_R) \quad (2)$$

$$\mathrm{OSD}P = logt_R - Q/[2.3R(T + 273.15)] \quad (3)$$

where t_R = time to rupture (h),
T = temperature (°C),
C, Q = optimized constants, and
R = gas constant.

There are also various time-temperature parameters not limited to the parameters mentioned above [26], the above two parameters are commonly and widely used. The master creep rupture curve equations for the fit were of the following form:

$$P = b_0 + b_1 logS + b_2 (logS)^2 + \ldots + b_k (logS)^k \quad (4)$$

where S = stress (MPa),
b_0, b_1, b_2, … b_k = regression coefficients estimated by the least squares method, and k = degree of regression equation.

Furthermore, region splitting analysis (RSA) method was also examined. RSA method was proposed to improve the accuracy of evaluation and prediction of long-term creep strength of CSEF steels. It evaluates creep data for high and low stress regimes independently, which is divided by 50% of 0.2% offset yield stress [27,28]. 50% of 0.2% offset yield stress corresponds to the elastic limit [29]. Even if creep test data at higher stresses above the elastic limit are extrapolated to lower stresses below the elastic limit, it is not possible to properly predict creep strength under elastic stress conditions. Therefore, it is considered that the accuracy of long-term creep strength predictions can be improved by analysing and

evaluating the high-stress and low-stress regimes independently, using 50% of 0.2% offset yield stress, which corresponds to the elastic limit, as a boundary condition. The results of the re-evaluation of the long-term creep strength using RSA method have been reflected in the review of allowable stress [8,18,19]. RSA method has also been employed to the extension of allowable stresses and design parameters for Grade 91 to support 60 years design life of high-temperature reactor [30,31].

4. Experimental results

4.1. Initial microstructure and tensile properties

Optical micrographs of the as-received samples are shown in Figure 2 (a) for tube steels, and (b) for plate and pipe steels. Microstructural observation area was a centre of the thickness for each sample. Horizontal axis of the micrographs corresponds to a longitudinal direction for tube and pipe steels, and a rolling direction for plate steels. Microstructure of the steels in the as-received condition is tempered martensite microstructure for all the sample. A certain amounts of delta ferrite phase with an elongated shape along rolling direction are observed for MgA and MgB heats of plate steels; however, it is scarcely observed for the other steels. An elongated shape of delta ferrite phase highly frequently observed at the centre of plate thickness is thought to be formed by rolling process.

Tensile strength properties of the Grade 91 steels are shown in Figure 3. Both 0.2% proof stress and tensile strength gradually decreases with increase in temperature up to about 400°C, and relatively large heat-to-heat variation of about 100 MPa is recognized in the same range of temperatures for 0.2% proof stress and tensile strength. In the range of temperatures at 500°C and above, both strength decreases with increase in temperature significantly compared to below 500°C, and differences in 0.2% proof stress and tensile strength among 11 heat steels are smaller than those in the lower temperatures at 400°C and below. Rupture elongation decreases slightly with increase in temperature up to about 400°C, and turns to increase above 400°C. On the other hand, reduction of area is almost constant at 400°C and below, it tends to increase at the higher temperature, as well as rupture elongation. No clear difference in tensile properties is observed for Grade 91 steels depending on the product form of tube, plate, and pipe.

4.2. Creep properties

Stress versus time to rupture of the Grade 91 steels over a range of temperatures from 450°C to 725°C is plotted in Figure 4. Slope of the relation between stress and time to rupture tends to steeper with decrease in

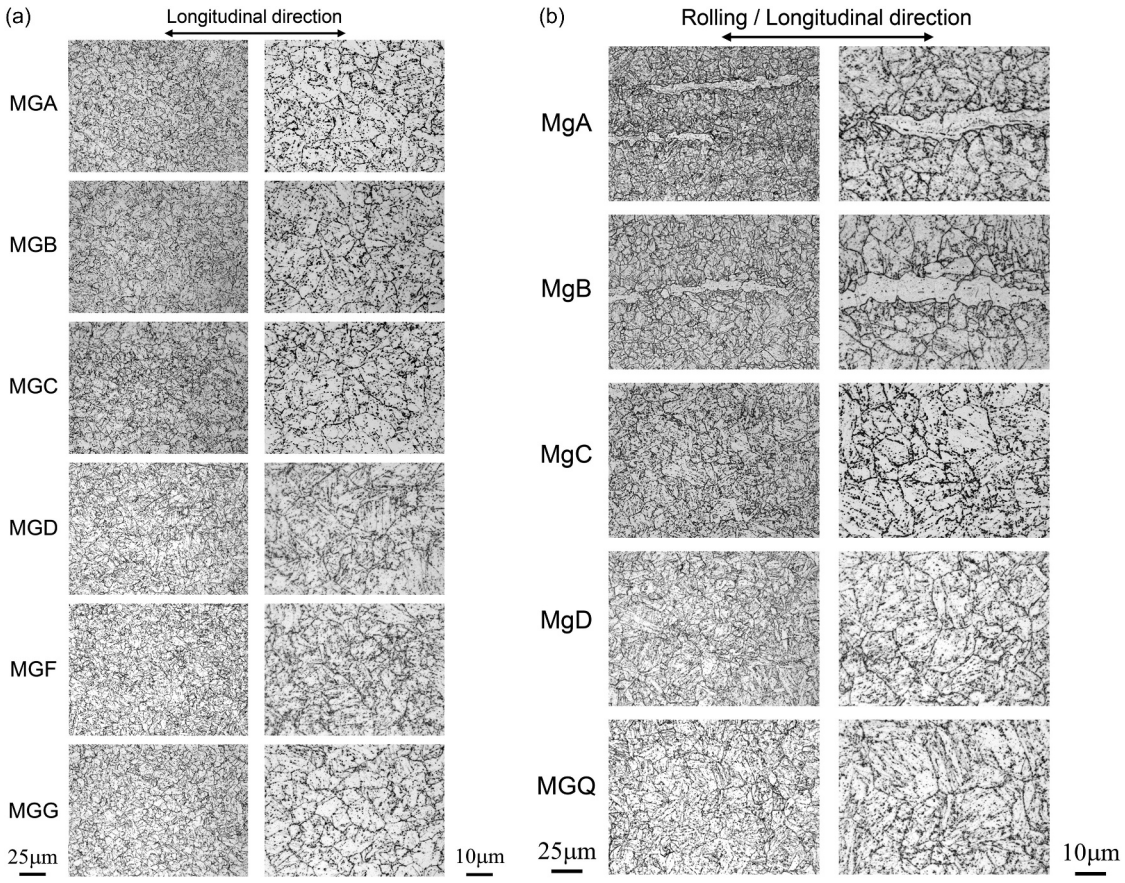

Figure 2. Optical micrographs of as-received 9Cr-1Mo-V-Nb steel (a) Tubes and (b) Plates and Pipe.

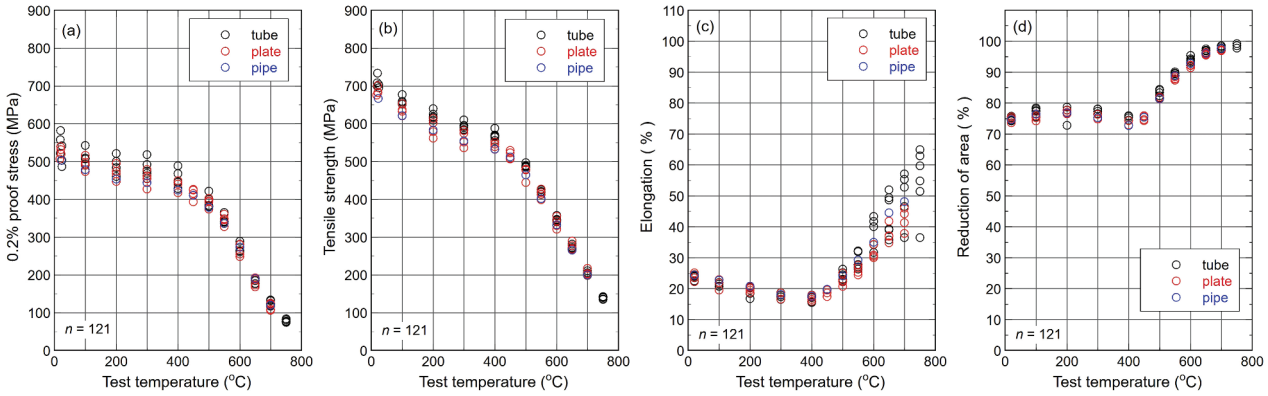

Figure 3. Tensile properties at various temperatures (a) 0.2% proof stress, (b) Tensile strength, (c) Elongation, and (d) Reduction of area.

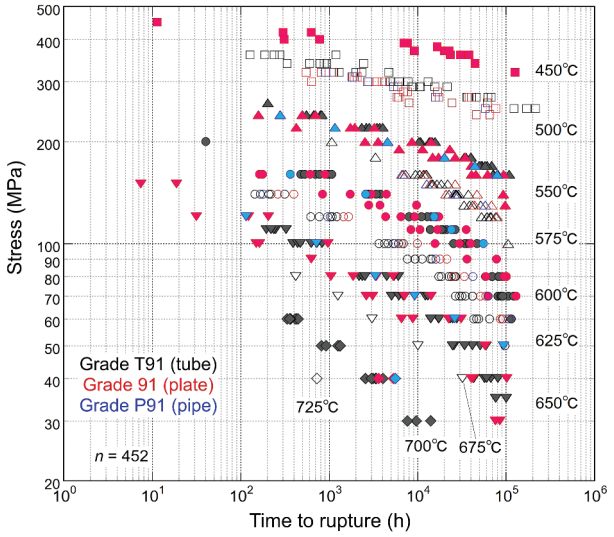

Figure 4. Creep rupture strength of 9Cr-1Mo-V-Nb steel tubes, plates and pipe.

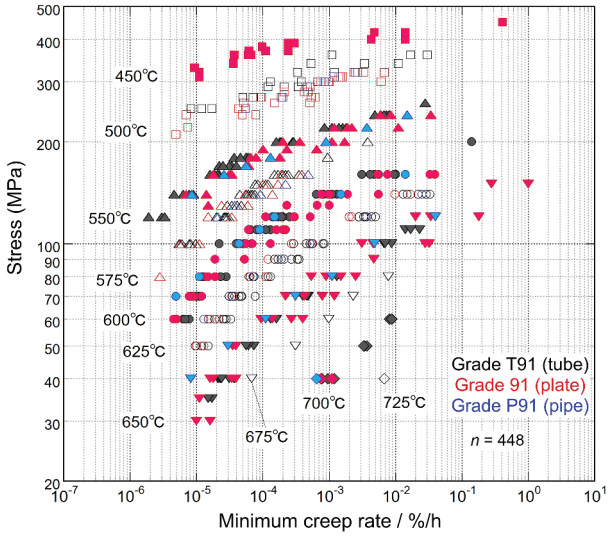

Figure 5. Stress versus minimum creep rate for 9Cr-1Mo-V-Nb steel tubes, plates and pipe.

stress, and remarkable drop in creep rupture strength is recognized in the long-term close to 100,000 h at 600°C and above. Heat-to-heat variation in time to rupture of about one order of magnitude is observed; therefore, range of time to rupture at 25°C different temperatures tend to overlap each other, especially in the long term at the higher temperature of 600°C and above.

Stress versus minimum creep rate of the Grade 91 steels over a range of temperatures from 450°C to 725°C is plotted in Figure 5. The stress dependence of minimum creep rate decreases with decrease in stress, and this stress dependence corresponds well to the time to rupture shown in Figure 4. The Monkman–Grant relationship [32] and the regression coefficient of the linear relationship are shown in Figure 6 and Table 3, respectively. Good linear relationship is observed over a wide range of time to rupture and minimum creep rate.

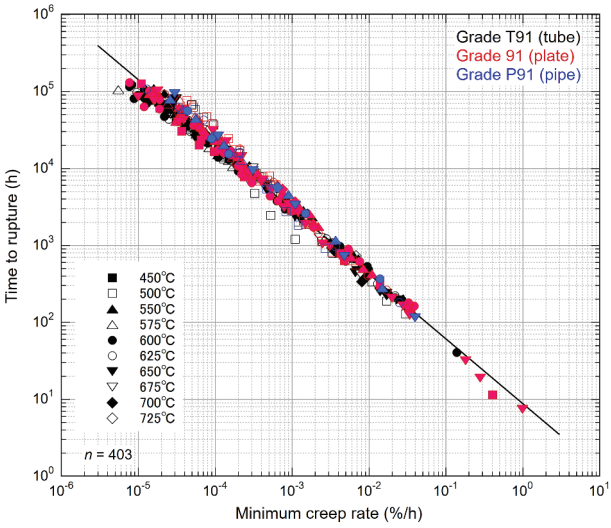

Figure 6. Monkman–Grant relations for 9Cr-1Mo-V-Nb steel tubes, plates and pipe.

Table 3. Regression coefficient of the linear relationship between time to rupture and minimum creep rate for 9Cr-1Mo-V-Nb steel tubes, plates and pipe.

			$\log t_R = A + B\log\dot{\varepsilon}_m$			
NIMS reference code	Product form	n^a	A	B	SEE	COD
MGA, MGB, MGC, MGD, MGF, MGG	Tube	220	9.594725×10^{-1}	-8.301514×10^{-1}	0.091	0.988
MgA, MgB, MgC, MgD	Plate	148	9.153267×10^{-1}	-8.566332×10^{-1}	0.101	0.987
MGQ	Pipe	35	8.155498×10^{-1}	-8.975373×10^{-1}	0.080	0.991
All steels	Tube/Plate/Pipe	403	9.401767×10^{-1}	-8.425420×10^{-1}	0.100	0.986

n : number of data points; SEE : standard error of estimate; COD : coefficient of determination; tR: time to rupture (h); em: minimum creep rate (%/h).

Rupture elongation and reduction of area for creep ruptured specimens of the Grade 91 steels are plotted against time to rupture and shown in Figures 7 and 8, respectively. Changes in creep rupture ductility with temperature and time are observed, especially it is more clearly recognized for reduction of area in Figure 8. In the temperature range below 575°C, creep ruptured specimens exhibit large reduction of area of over 60%; however, it slightly tends to decrease with increase in time in the long term. Although a large reduction of area of over 80% is observed in the short-term range of 10,000 h or less, remarkable drop in the reduction of area is clearly recognized in the long term at the temperature range between 600°C and 675°C. Minimum value of reduction area, that is less than 20%, is observed at 650°C. On the other hand, such remarkable drop in creep rupture ductility is not observed at 700°C and 725°C. Significant decrease in rupture ductility is a major concern, because sufficiently high creep rupture ductility is necessary to maintain the integrity and reliability of high temperature structural components. Several causes have been proposed to reduce creep rupture ductility. Precipitation of Laves phase and its coarsening is reported as a cause of ductility drop, since many cavities are nucleated at coarse Laves phase particles on grain boundaries [12]. The effects of harmful elements such as aluminium, arsenic, antimony, tin, etc., on the ductility drop has also been reported [33–35]. Based on those findings, material specification with strict restrictions on impurity elements, etc., has been developed as Grade 91 Type 2, to suppress the remarkable drop in creep rupture ductility [20]. On the other hand, inhomogeneous recovery of tempered martensitic microstructure in the vicinity of prior austenite grain boundary is also proposed as a candidate cause of ductility drop, because remarkable drop in rupture ductility is recognized in the stresses just below 50% of 0.2% proof stress that correspond to the elastic limit and ductility tends to increase in the long term after showing temporary drop [36]. The underlying principle of this idea is closely related to RSA method of creep data analysis.

4.3. Microstructure of creep-ruptured samples

Optical micrographs of the gauge portion of creep ruptured specimens at 500, 550, 600, and 650°C are shown in Figure 9 (a) tube steels, and (b) plate and pipe steels. The specimens with the longest

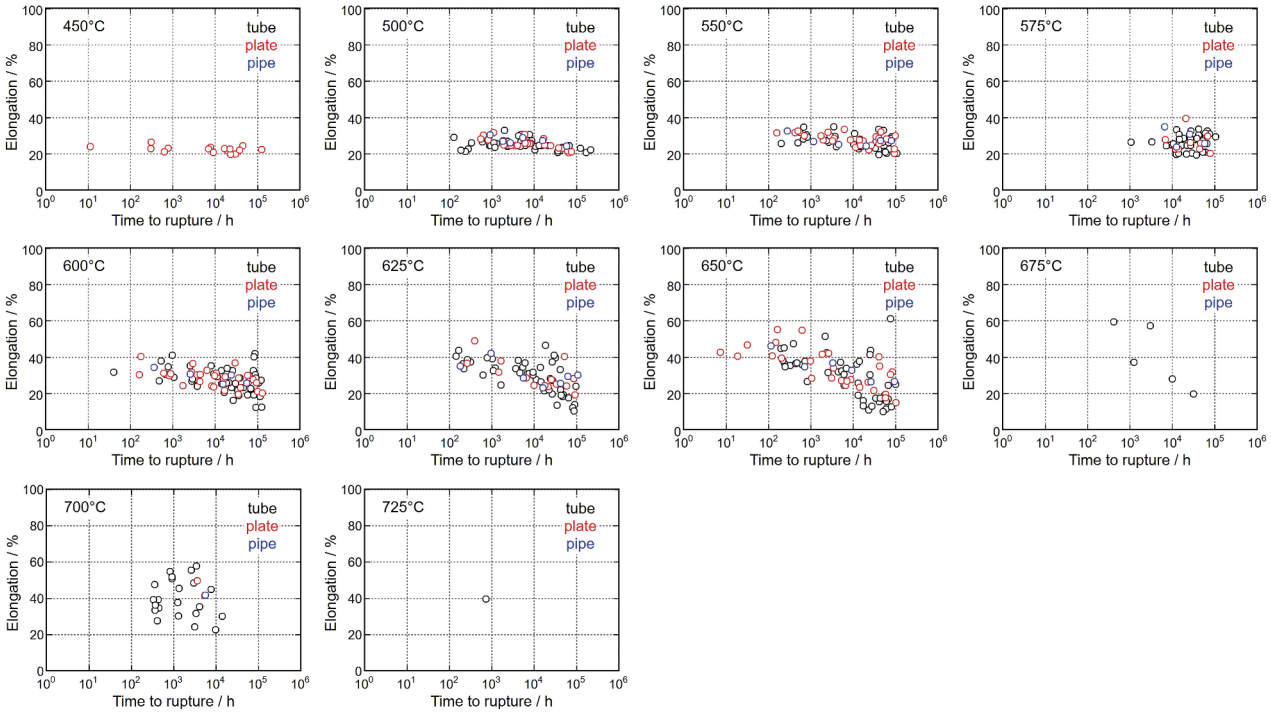

Figure 7. Rupture elongation of creep ruptured samples over a range of temperatures from 450 to 725°C.

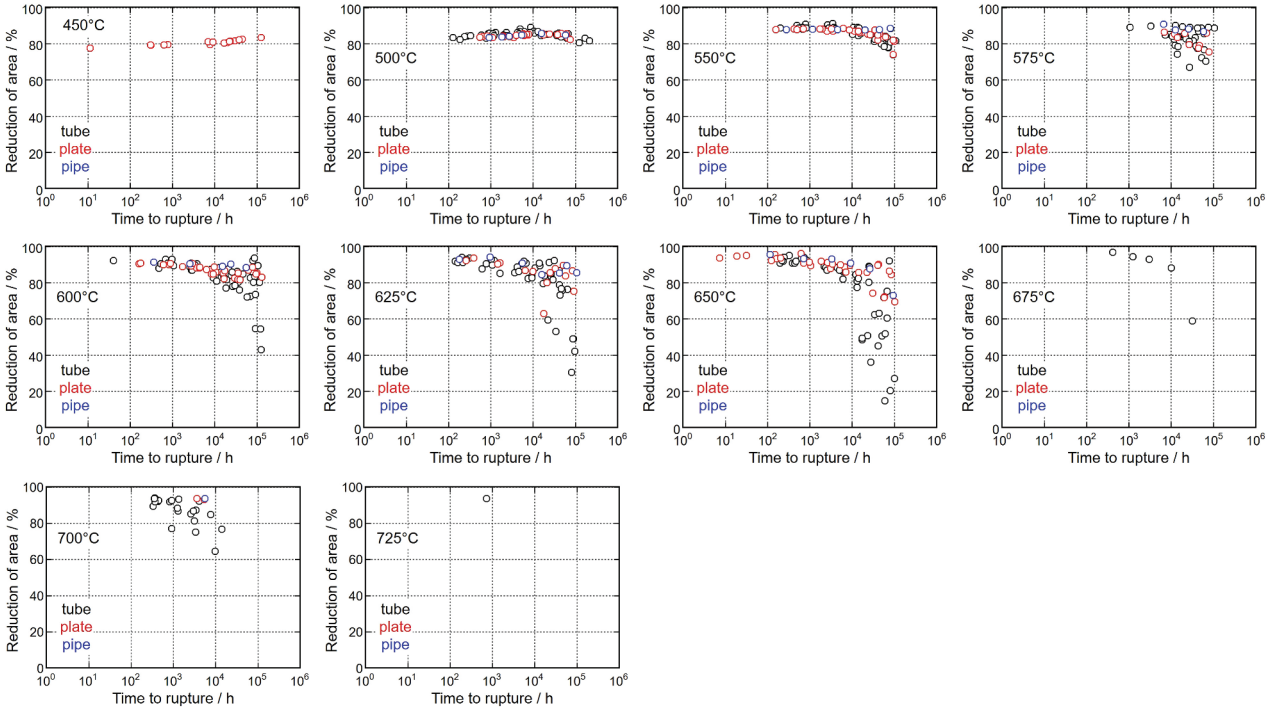

Figure 8. Reduction of area of creep ruptured samples over a range of temperatures from 450 to 725°C.

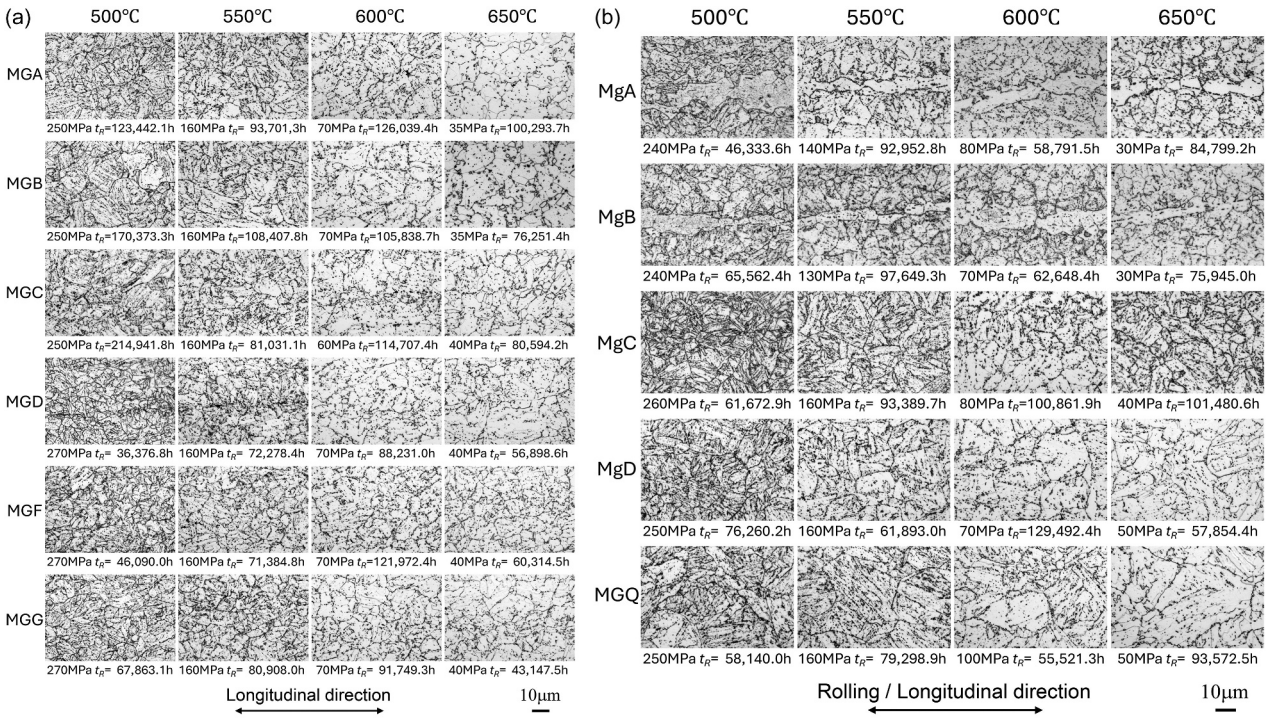

Figure 9. Optical micrographs of gauge portion of creep ruptured samples of (a) Tubes and (b) Plates and pipe steels.

time to rupture at each temperature were selected for microstructural observation. Horizontal axis of the micrographs corresponds to a longitudinal direction for tube and pipe steels, and a rolling direction for plate steels. With increase in testing temperature, coarsening and decrease in number density of precipitate particles become clearly recognizable, and the disappearance of boundaries such as block and lath becomes apparent. Delta ferrite phase observed in the as-received condition of MgA and MgB heats of plate steels are still clearly observed in the creep ruptured specimens after long-term creep exposure at the elevated temperatures.

5. Analysis of experimental data

5.1. Analysis of short-term tensile data

Results of the regression analysis on the short-term tensile data of 0.2% proof stress and tensile strength are shown in Figure 10 for each product form of tube, plate, and pipe steels. The third, fourth, and fifth order of a regression Equation (1) were used to express the temperature dependence of the 0.2% proof stress and tensile strength. The fitting curve with third order shows a tendency to overestimate 0.2% proof stress of the plate and pipe steels in the range of temperatures between 300 and 450°C. However, such a tendency of overestimation is not observed for 0.2% proof stress of tube steels, and the fitting curves with third and fourth order are almost the same each other. On the other hand, no clear difference is observed, and similar results are obtained for all orders of the fitting curves for tensile strength. According to the principle of choosing the lower order if the accuracy is the same level, the fitting curve with third order was selected for 0.2% proof stress of tube steel and tensile strength of tube, plate, and pipe steels, and the fitting curve with fourth order was selected for 0.2% proof stress of plate and pipe steels. The regression coefficients for the selected fitting curves are listed in Table 4.

5.2. Analysis of creep rupture data

In this section, creep rupture life was examined by six-type data analysis procedures. Generally, Time-Temperature-Parameter (TTP) method is used for estimation of long-term creep strength by extrapolating short-term creep test data. The basic concept of creep data analysis with TTP method is a temperature compensation based on the assumption that short-term creep rupture life at the higher temperature corresponds to long-term creep rupture life at the lower temperature and the same stress condition. On the other hand, concerns have been reported that traditional TTP methods may result in overestimation for long-term creep strength of CSEF steels [2–4]. It has been reported that a progress in microstructural change in Grade 91 steel is different in high- and low-stress regimes which is divided by about 50% of 0.2% proof stress at the temperatures and, therefore, this

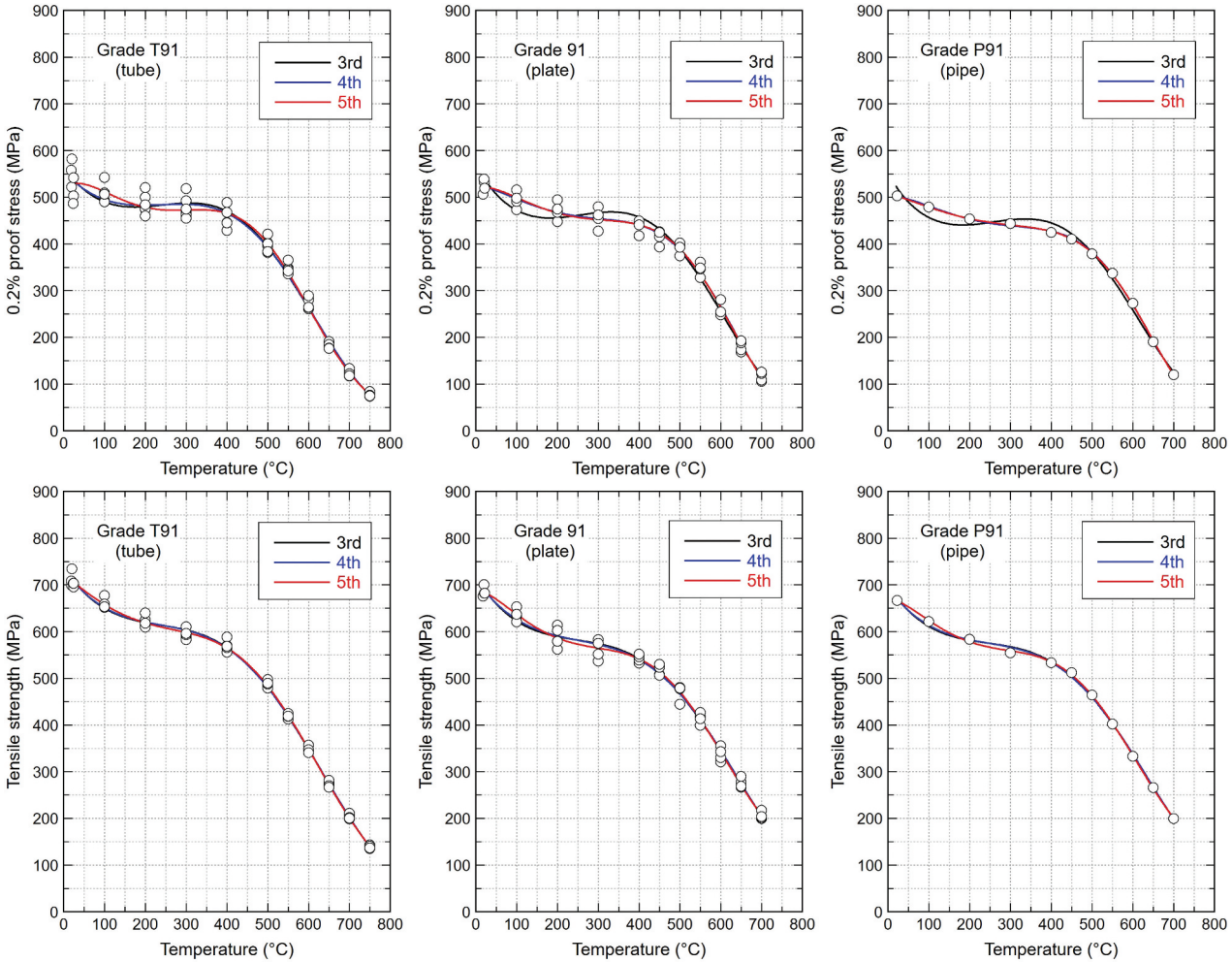

Figure 10. Result of regression analysis of third, fourth and fifth degree for 0.2% proof stress and tensile strength, for 9Cr-1Mo-V-Nb steel tubes, plates and pipe.

Table 4. Summary of polynomial regression for short-term tensile properties for 9Cr-1Mo-V-Nb steel tubes, plates and pipe.

NIMS reference code	Product form	Dependent Variable	n	$log(S_y or S_T) = a_0 + a_1T + a_2T^2 + a_3T^3 + a_4T^4$						
				a_0	a_1	a_2	a_3	a_4	SEE	COD
MGA, MGB	Tube	$logS_y$	66	2.7539	-1.0376×10^{-3}	4.6529×10^{-6}	-6.4261×10^{-9}	–	0.023	0.993
MGC, MGD		$logS_T$	66	2.8691	-8.2957×10^{-4}	3.0932×10^{-6}	-4.3692×10^{-9}	–	0.008	0.999
MGF, MGG										
MgA, MgB	Plate	$logS_y$	44	2.7229	-1.7056×10^{-4}	-1.7760×10^{-6}	8.7174×10^{-9}	-1.1117×10^{-11}	0.021	0.990
MgC, MgD		$logS_T$	44	2.8572	-9.1492×10^{-4}	3.2803×10^{-6}	-4.4094×10^{-9}	–	0.014	0.993
MGQ	Pipe	$logS_y$	11	2.7023	-3.9944×10^{-5}	-2.5146×10^{-6}	1.0172×10^{-8}	-1.1890×10^{-11}	0.005	1.000
		$logS_T$	11	2.8454	-8.6953×10^{-4}	3.1996×10^{-6}	-4.3919×10^{-9}	–	0.006	0.999

n : number of data points. SEE : standard error of estimate. COD: coefficient of determination. S_y : 0.2% offset yield stress (MPa). S_T : tensile strength (MPa).

difference in microstructural evolution during creep exposure has been considered as a cause of overestimation for long-term creep strength of CSEF steels [4]. By considering this discontinuous effect of stress on creep strength property of CSEF steels, a region splitting analysis (RSA) method [27,28] which evaluates creep strength in high- and low-stress regimes separately was proposed as a reliable, useful and easy analysis method. RSA method has already been used to review allowable stresses of CSEF steels [8,18,19] and to develop design parameters for Grade 91 to support 60 years design life of high temperature reactor [30,31]. Considering the above points, two type Time-Temperature-Parameter (TTP) of Larson-Miller (LM) [24] and Orr-Sherby-Dorn (OSD) [25] parameters were used for regression analysis with second and third-order regression equations of logarithm stress. Although a wide variety of Time-Temperature-Parameters are investigated [26], the LM and OSD parameters are used in this study, because these two parameters are commonly and widely used for creep rupture data analysis. In addition, the creep strength evaluation by means of region splitting analysis [27,28] with using LM parameter is also examined.

Results of regression analysis on time to rupture are shown in Figure 11 for LM parameter with (a) second and (b) third order polynomials, OSD parameter with (c) second and (d) third order polynomials, and by means of region splitting analysis method with LM parameter and (e) second and second order polynomials, and (f) third and second order polynomials for high- and low-stress regimes, respectively. The coefficients obtained by regression analysis on time to rupture are listed in Table 5, together with the standard error of the estimate and coefficient of determination. For both LM and OSD parameters, second order

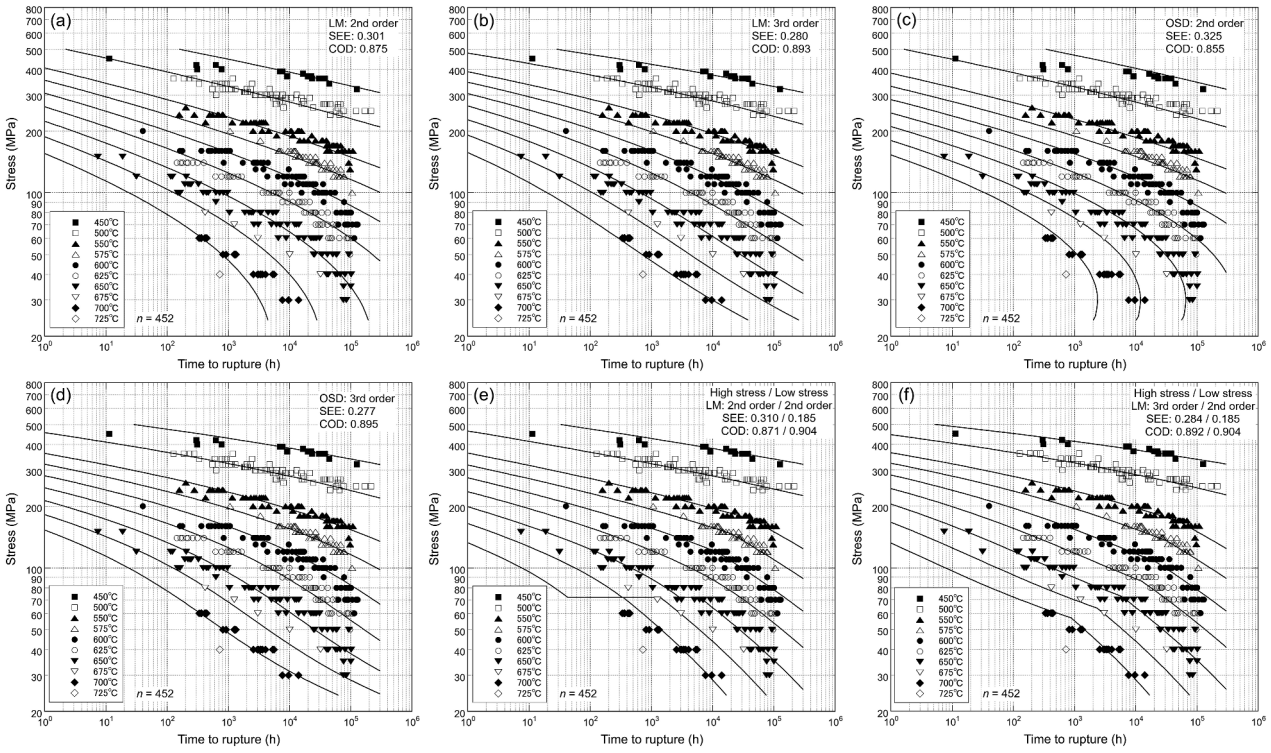

Figure 11. Result of regression analysis on time to rupture by Larson-Miller parameter with (a) second and (b) third order polynomials, Orr-Sherby-Dorn parameter with (c) second and (d) third order polynomials and by means of region splitting method with Larson-Miller parameter and (e) second and second order polynomials, and (f) third and second order polynomials for high- and low-stress regimes, respectively.

Table 5. Summary of regression coefficient of Larson-Miller and Orr-Sherby-Dorn parameters for creep rupture data.

Larson-Miller : $logt_R = (T+273.15)^{-1}\left[b_0 + b_1 logS + b_2(logS)^2 + b_3(logS)^3\right] - C$

Orr-Sherby-Dorn : $logt_R = Q[2.3R(T+273.15)]^{-1} + b_0 + b_1 logS + b_2(logS)^2 + b_3(logS)^3$

TTP	Stress regime	n	Order of regression	C	Q	b_0	b_1	b_2	b_3	SEE	COD
LM	All	452	2nd	26.54879	–	22,671.292	10,685.783	−4,216.807	–	0.301	0.875
			3rd	26.82501	–	57,692.441	−40,766.58	20,840.223	−4,019.286	0.280	0.893
OSD			2nd	–	495,713.36	−37.88072	19.81471	−6.7143557	–	0.325	0.855
			3rd	–	511,850.23	21.826053	−70.54813	37.652176	−7.184197	0.277	0.895
LM	High	207	2nd	32.11343	–	15,590.058	22,631.509	−7,185.964	–	0.310	0.871
			3rd	31.19382	–	141,824.00	−148,593.515	69,222.827	−11,288.906	0.284	0.892
	Low	245	2nd	20.46611	–	25,558.22	633.0300	−1,261.066	–	0.185	0.904

n: number of data points. SEE: standard error of estimate. COD: coefficient of determination. t_R: time to rupture (h). T: temperature (°C). S: stress (MPa). R: gas constant.

polynomial of logarithm stress gives a predict result of significant decrease in creep rupture strength in the low stress regime (Figure 11(a,c)), especially 100,000 h creep rupture strength at 650°C cannot be obtained by OSD parameter with second order polynomial due to turn back of regression curve in the low stresses. On the other hand, the regression curves obtained by third order polynomials of both LM and OSD parameters bend upward in the low stresses; therefore, the risk of overestimation of long-term creep rupture strength should be considered (Figure 11(b,d)). An unnatural and inaccurate shape of the regression curve is observed for the analysis result by means of RSA method and LM parameter with both second order polynomials for high- and low-stress regimes (Figure 11(e)). The two curves obtained for high- and low-stress regimes do not intersect each other in the temperature range above 650°C; therefore, stress versus time to rupture curve indicates discontinuous shape with a step as shown in Figure 11(e). Creep rupture data are evaluated with high accuracy in all temperature and stress ranges, by means of RSA method and LM parameter with third and second order polynomials for high- and low-stress regimes (Figure 11(f)). From the perspective of statistical indicators that the smallest number of standard error of estimate (SEE) and the largest number of coefficient of determination (COD) for low-stress regime with RSA method as listed in Table 5, the advantage of RSA method over full data analysis for long-term creep rupture life evaluation is suggested.

In order to examine the availability of the analysis procedures, predicted creep rupture life obtained by six-type data analysis procedures is plotted against observed creep rupture life and shown in Figure 12. For RSA method, creep rupture data in the high- and

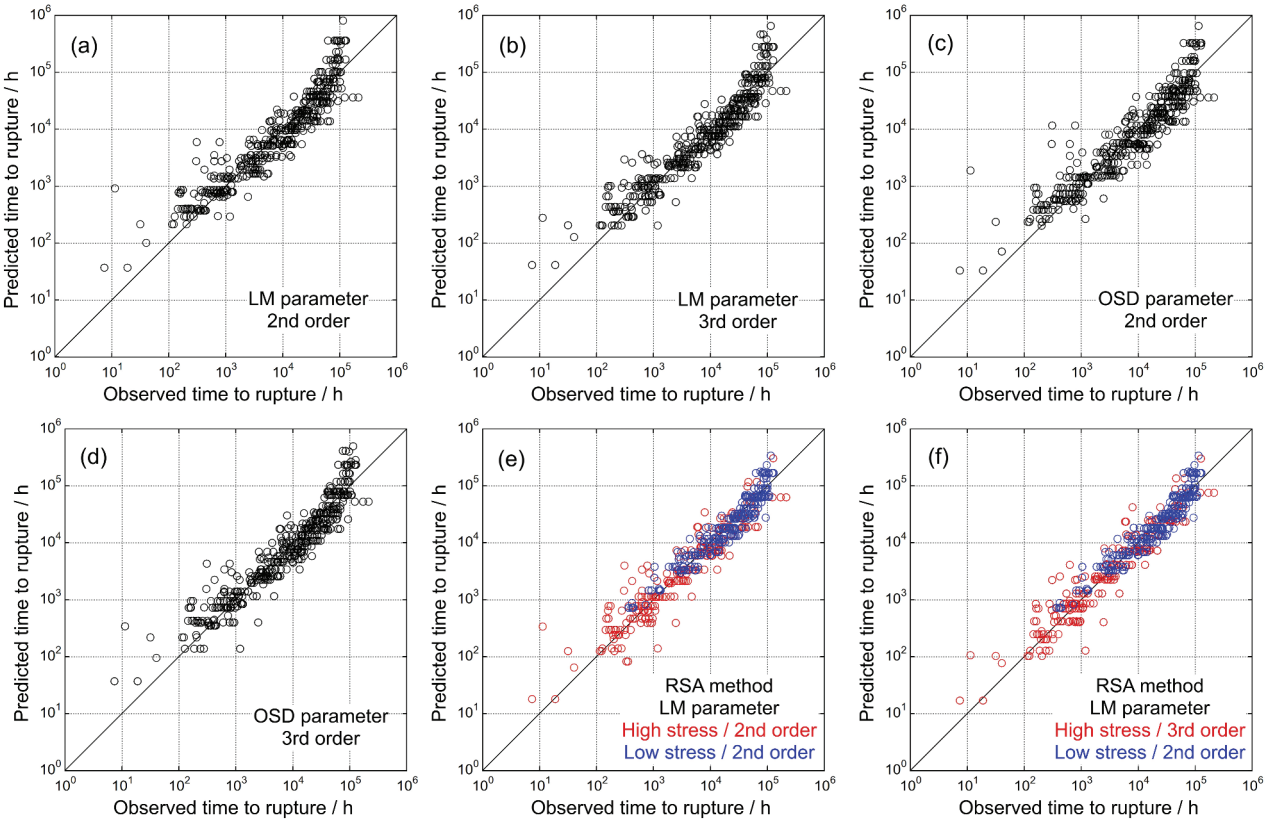

Figure 12. Comparison of observed and predicted time to rupture obtained by regression analysis shown in Figure 11.

low-stress regimes are illustrated by red and blue symbols, respectively. In the top and right corner of Figure 12(a–d) for full data analysis, many data plots are observed to deviate significantly above the 45° line. This upward deviation indicates that the predicted creep rupture lives are overestimated in the long term. Compared to these upward deviations observed for full data analysis, the deviation of the data plot predicted by RSA method in the long term is small, as shown in Figure 12(e,h). In addition, the deviation of the data plot predicted by RSA method with third order polynomial in the high-stress and short-term regime (Figure 12(f)) is the smallest among the six procedures studied. 50% of the 0.2% offset yield stress used as the boundary stress condition in the RSA method corresponds to the elastic limit. Unlike the high-stress regime where plastic deformation due to applied stress above the elastic limit contributes significantly, the influence of diffusion controlled microstructural changes on creep deformation behaviour becomes apparent in the low-stress regime below the elastic limit. As mentioned in the Introduction, several factors that cause creep strength degradation have been reported, most of them are closely related to microstructural changes during creep exposure at the elevated temperatures, and such a degradation is caused by microstructural changes controlled by diffusion. Therefore, by analysing creep test data separately for the stress regimes above and below the elastic limit, the effects of material degradation can be properly analyzed and evaluated. The evaluated 100,000 h creep rupture strength at 550, 575, 600, 625, and 650°C with the different procedures are listed in Table 6. Since the difference in two-type RSA methods is the order of polynomial for high-stress regime, 100,000 h creep rupture strength evaluated from the low-stress regime is the same value. Evaluating the 100,000 h creep rupture strength by means of the RSA method is the lower than those values obtained by full data analysis except at 550°C, evaluated strength of 150MPa at 550°C of RSA method is comparable to other values in the range of 148 to 154MPa. Compared to the results of analyzing all data at once without dividing the data into regimes, the analytical results of the RSA method are more conservative and can prevent overestimating the long-term creep strength. From the above results, it is concluded that a result of evaluation by means of RSA method with third and second order polynomials for high- and low-stress regimes, respectively, is the most appropriate and accurate.

Creep rupture data were evaluated using LM parameter by means of RSA method with third and second order polynomials for high- and low-stress regimes, respectively, for each product form of tube, plate, and pipe steels, and the results of regression analysis are shown in Figure 13 (a) tubes, (b) plates, and (c) pipe steels. The corresponding regression coefficients are listed in Table 7. The regression curves are displayed within the stress range of the data analysed. Good correspondence between data plots and the regression curves are observed within the entire temperature and

Table 6. Summary of 100,000 h creep rupture strength evaluated by Larson-Miller and Orr-Sherby-Dorn parameters for creep rupture data with and without region splitting analysis method.

			100,000 h creep rupture strength/MPa				
TTP	Stress regime	Order of regression	550°C	575°C	600°C	625°C	650°C
LM	All	2^{nd}	149	116	87	60	35
		3^{rd}	153	116	84	58	39
OSD		2^{nd}	148	115	86	60	NA
		3^{rd}	154	116	83	56	38
LM	RSA	2^{nd}– 2^{nd} 3^{rd}-2^{nd}	150	110	78	54	35

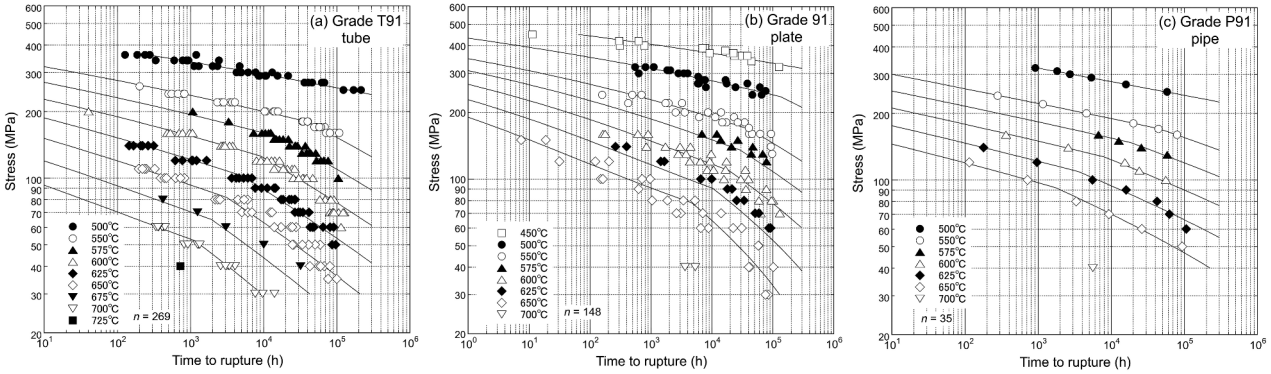

Figure 13. Selected fitting curves by means of region splitting analysis with Larson-Miller parameter listed in Table 7, for 9Cr-1Mo-V-Nb steel (a) Tubes, (b) Plates and (c) Pipe.

Table 7. Summary of regression coefficient of Larson-Miller parameter with region splitting method for 9Cr-1Mo-V-Nb steel tubes, plates and pipe.

NIMS reference code	Product form	Stress regime	$logt_R = (T+273.15)^{-1}\left[b_0 + b_1 logS + b_2(logS)^2 + b_3(logS)^3\right] - C$							
			n	C	b_0	b_1	b_2	b_3	SEE	COD
MGA, MGB MGC, MGD	Tube	High	109	36.09361	7.658599×10^4	-4.899833×10^4	2.259875×10^4	-4.144382×10^3	0.158	0.965
MGF, MGG		Low	160	20.77372	2.771036×10^4	-1.369250×10^3	-7.347882×10^2	–	0.150	0.945
MgA, MgB MgC, MgD	Plate	High	80	32.89420	1.618852×10^5	-1.700228×10^5	7.748949×10^4	-1.237721×10^4	0.313	0.890
		Low	68	19.32610	2.220923×10^4	2.933414×10^3	-1.824122×10^3	–	0.235	0.801
MGQ	Pipe	High	18	36.96826	2.873014×10^4	2.425777×10^4	-1.321099×10^4	1.546090×10^3	0.044	0.998
		Low	17	26.18250	3.114645×10^4	2.072207×10^3	-2.086992×10^3	–	0.107	0.956

n : number of data points. SEE : standard error of estimate. COD : coefficient of determination. t_R : time to rupture (h). T : temperature (°C). S : stress (MPa).

stress range, except for creep test data at 625°C of plate steels. This discrepancy between data plots and the regression curve is caused by considerable large heat-to-heat variation of creep strength among four heats of plate steels. Creep rupture strength of MgA and MgB heats is quite low in comparison with those of MgC and MgD heats, due to a presence of certain amounts of delta ferrite phase in MgA and MgB heat as shown in Figure 9(b) [14]. All the creep test data at 625°C of plate steels are obtained for MgC and MgD heats, therefore, the data plots at 625°C appears to be shifted to the high strength side of the regression curve. Temperature dependence of the 0.2% proof stress, tensile strength, and creep rupture strength at 100, 1,000, 10,000, and 100,000 h estimated from the regression equations listed in Tables 4 and 7 are shown in Figure 14 (a) tube, (b) plate, and (c) pipe steels. The creep rupture strength estimated using the regression coefficients listed in Table 7 are shown in Table 8 (a) tube, 8 (b) plate, and 8 (c) pipe steels. The

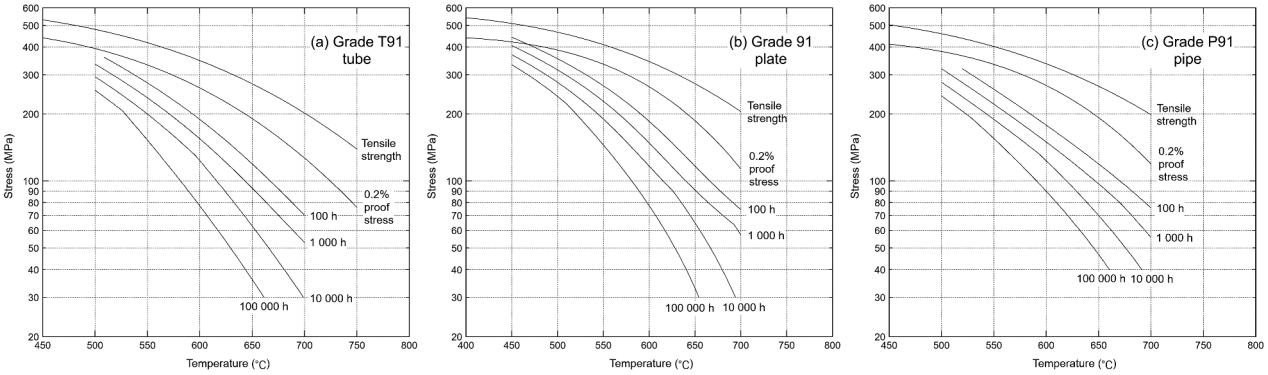

Figure 14. Temperature dependence of 0.2% proof stress, tensile strength and creep rupture strength at 100, 1000, 10,000 and 100,000 h, for 9Cr-1Mo-V-Nb steel (a) Tubes, (b) Plates and (c) Pipe.

Table 8(a). Summary of creep rupture strength in MPa evaluated from curvilinear regression using Larson-Miller parameter with region splitting method for 9Cr-1Mo-V-Nb steel tubes.

NIMS reference code	Number of data points	500°C			525°C				550°C			
		10^3 h	10^4 h	10^5 h	10^2 h	10^3 h	10^4 h	10^5 h	10^2 h	10^3 h	10^4 h	10^5 h
MGA, MGB MGC, MGD MGF, MGG	269	335	294	256	325	284	245	209	276	236	200	153

NIMS reference code	Number of data points	575°C			600°C				625°C				
		10^2 h	10^3 h	10^4 h	10^5 h	10^2 h	10^3 h	10^4 h	10^5 h	10^2 h	10^3 h	10^4 h	10^5 h
MGA, MGB MGC, MGD MGF, MGG	269	231	193	160	110	189	155	124	77	152	121	89	54

NIMS reference code	Number of data points	650°C			675°C				700°C		
		10^2 h	10^3 h	10^4 h	10^5 h	10^2 h	10^3 h	10^4 h	10^2 h	10^3 h	10^4 h
MGA, MGB MGC, MGD MGF, MGG	269	120	93	63	36	92	70	44	70	53	30

Table 8(b). Summary of creep rupture strength in MPa evaluated from curvilinear regression using Larson-Miller parameter with region splitting method for 9Cr-1Mo-V-Nb steel plates.

NIMS reference code	Number of data points	450°C				475°C				500°C				525°C			
		10^2 h	10^3 h	10^4 h	10^5 h	10^2 h	10^3 h	10^4 h	10^5 h	10^2 h	10^3 h	10^4 h	10^5 h	10^2 h	10^3 h	10^4 h	10^5 h
MgA, MgB MgC, MgD	148	443	406	369	333	398	361	323	286	354	316	278	240	311	272	233	190
NIMS reference code	Number of data points	550°C				575°C				600°C				625°C			
		10^2 h	10^3 h	10^4 h	10^5 h	10^2 h	10^3 h	10^4 h	10^5 h	10^2 h	10^3 h	10^4 h	10^5 h	10^2 h	10^3 h	10^4 h	10^5 h
MgA, MgB MgC, MgD	148	268	228	190	145	226	187	150	108	185	148	117	77	148	116	91	53
NIMS reference code	Number of data points	650°C				675°C			700°C								
		10^2 h	10^3 h	10^4 h	10^5 h	10^2 h	10^3 h	10^4 h	10^2 h	10^3 h							
MgA, MgB MgC, MgD	148	117	91	65	33	92	73	44	74	57							

Table 8(c). Summary of creep rupture strength in MPa evaluated from curvilinear regression using Larson-Miller parameter with region splitting method for 9Cr-1Mo-V-Nb steel pipe.

NIMS reference code	Number of data points	500°C			525°C				550°C			
		10^3 h	10^4 h	10^5 h	10^2 h	10^3 h	10^4 h	10^5 h	10^2 h	10^3 h	10^4 h	10^5 h
MGQ	35	320	278	241	308	267	230	198	258	221	189	155
NIMS reference code	Number of data points	575°C				600°C				625°C		
		10^2 h	10^3 h	10^4 h	10^5 h	10^2 h	10^3 h	10^4 h	10^5 h	10^2 h	10^3 h	10^4 h	10^5 h
MGQ	35	215	183	154	119	178	150	123	90	147	121	94	66
NIMS reference code	Number of data points	650°C				675°C			700°C				
		10^2 h	10^3 h	10^4 h	10^5 h	10^2 h	10^3 h	10^4 h	10^2 h	10^3 h			
MGQ	35	119	97	70	47	96	76	51	76	56			

minimum creep rate data shown in Figure 5 are evaluated and fitted to a regression equation of logarithm stress using LM parameter by means of RSA method with third and second order polynomial for high- and low-stress regimes, respectively, in the same manner as the time to rupture. The evaluated fitting master curves and regression coefficients are shown in Figure 15 (a) tube, (b) plate, and (c) pipe steels and Table 9.

The data tables used in the present study will be published in a database at https://cds.nims.go.jp/ as a NIMS Creep Data Sheet.

6. Conclusions

Short-term tensile and creep rupture data were obtained for 11 heats of 9Cr-1Mo-V-Nb steel tubes, plates and pipe steels (ASME Grade T91 Type 1, Grade 91 Type 1, and Grade P91 Type1, respectively). Regression analysis for creep rupture data was performed using Larson-Miller and Orr-Sherby-Dorn parameters with second and third order polynomials of logarithm stress, and region splitting analysis method was also examined using Larson-Miller parameter with second and third order polynomials for high-stress regime and second order polynomial for low-stress regime. The result of

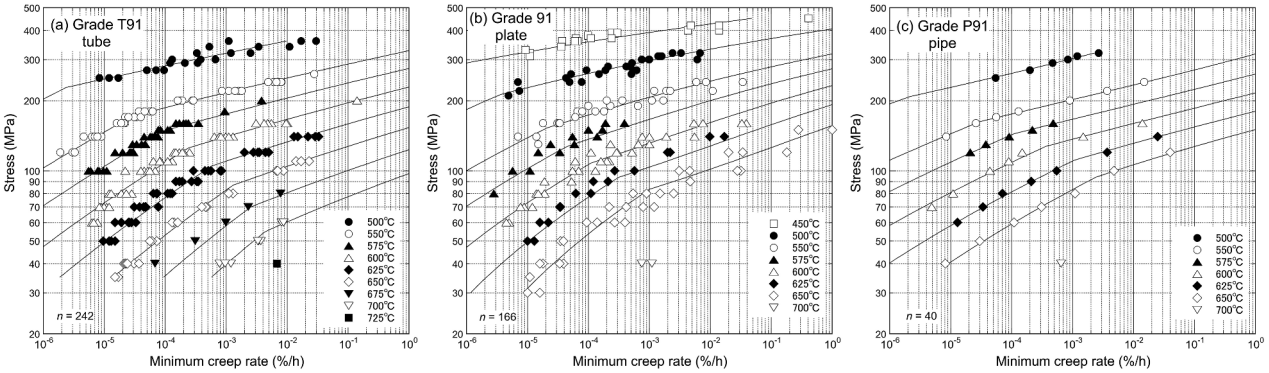

Figure 15. Stress versus minimum creep rate for 9Cr-1Mo-V-Nb steels (a) Tubes, (b) Plates and (c) Pipe. The regression coefficients are given in Table 8.

Table 9. Regression coefficients of Larson-Miller parameter for minimum creep rate data for 9Cr-1Mo-V-Nb steel tubes, plates and pipe.

NIMS reference code	Product form	Stress regime	$log\dot{e}_m = (T+273.15)^{-1}\left[d_0 + d_1 logS + d_2(logS)^2 + d_3(logS)^3\right] - C$							
			n	C	d_0	d_1	d_2	d_3	SEE	COD
MGA, MGB	Tube	High	87	−43.25105	-4.806372×10^4	-3.456799×10^3	2.890537×10^3	1.804780×10^2	0.229	0.946
MGC, MGD		Low	155	−26.51684	-3.287088×10^4	8.830962×10^2	1.069077×10^3	–	0.141	0.968
MGF, MGG										
MgA, MgB	Plate	High	85	−37.53935	-1.848147×10^5	1.920925×10^5	-8.607378×10^4	1.354424×10^4	0.388	0.889
MgC, MgD		Low	81	−25.98969	-2.920114×10^4	-2.678168×10^3	2.055960×10^3	–	0.208	0.915
MGQ	Pipe	High	18	−41.71294	6.749454×10^4	-1.648071×10^5	7.834313×10^4	-1.148587×10^4	0.071	0.995
		Low	22	−30.23701	-3.599495×10^4	-1.005481×10^3	1.966067×10^3	–	0.090	0.984

n : number of data points. SEE : standard error of estimate. COD : coefficient of determination. $\dot{e}_m$: minimum creep rate (%/h). T : temperature (°C). S : stress (MPa).

creep rupture data evaluation using Larson-Miller parameter by means of RSA method with third and second order polynomials for high- and low-stress regimes, respectively, was the most appropriate and accurate, and temperature dependence of creep rupture strength at 100, 1,000, 10,000, and 100,000 h were evaluated for tube, plate, and pipe steels. Minimum creep rate data was also evaluated by the same manner as time to rupture by means of RSA method, using Larson-Miller parameter with third and second order polynomials for high- and low-stress regimes, respectively.

Disclosure statement

No potential conflict of interest was reported by the author(s).

References

[1] Masuyama F. History of power plants and progress in heat resistant steels. ISIJ Int. 2001;41(6):612–625. doi: 10.2355/isijinternational.41.612

[2] Foldyna V, Kuboň Z, Jakobová A, et al. Development of advanced high chromium ferritic steels. Microstructural development and stability in high chromium ferritic power plant steels. In: Strang A, Gooch D, editors. Microstructure of high temperature materials number 1. London (UK): The Institute of Materials; 1997. p. 73–92.

[3] Strang A, Vodárek V. Microstructural stability of creep resistant martensitic 12%Cr steels. Microstructural stability of creep resistant alloys for high temperature plant applications. In: Strang A, Cawley J, Greenwood G, editors. Microstructure of high temperature materials number 2. London (UK): The Institute of Materials; 1998. p. 117–133.

[4] Kimura K, Kushima H, Abe F. Heterogeneous changes in microstructure and degradation behaviour of 9Cr-1Mo-V-Nb steel during long term creep. Kem. 2000;171–174:483–490. doi: 10.4028/www.scientific.net/KEM.171-174.483

[5] Brett SJ, Allen DJ, Pacey J. Failure of a modified 9Cr header endplate. In: Bicego V, Nitta A, Price JWH, Viswanathan R, editors. Proceedings International Symposium on Case Histories on Integrity and Failures in Industry; 1999; Milan, Italy. West Midlands (UK): Engineering Materials Advisory Services Ltd. p. 873–884.

[6] Brett SJ. Identification of weak thick section modified 9Cr forgings in service. In: Viswanathan R, Bakker WT, Parker JD, editors. Proceedings 3rd Conference Advances in Material Technology for Fossil Power Plants; 2001; Swansea, UK. London (UK): The Institute of Materials. p. 343–351.

[7] Brett SJ, Oates DL, Johnston C. In-service type IV cracking in a modified 9Cr (grade 91) header. In: Shibli IA, Holdsworth SR, Merckling G, editors. Proceedings Creep & Fracture in High Temperature Components – Design & Life Assessment Issues; 2005; London, UK. Pennsylvania (USA): DEStech Publications, Inc. p. 563–572.

[8] Yoshida K, Nakai H, Fukuda M. Regulatory review results on allowable tensile stress values of creep strength enhanced ferritic steels. Proc CREEP2007. 2007:CREEP2007–26512. doi: 10.1115/CREEP2007-26512

[9] Hofer P, Cerjak H, Schaffernack B, et al. Quantification of precipitates in advanced creep resistant 9–12% Cr steels. Steel Res. 1998;69(8):343–348. doi: 10.1002/srin.199805562

[10] Kimura K, Kushima H, Abe F, et al. Microstructural change and degradation behaviour of 9Cr-1Mo-V-Nb steel in the long term region. In: Strang A, Banks WM, Conroy RD, McColvin GM, Neal JC, Simpson S, editors. Proceedings 5th Intern Charles Parsons Turbine Conference; 2000; Cambridge, UK. London (UK): IOM Communications Ltd. p. 590–602.

[11] Strang A, Foldyna V, Lenert J, et al. Prediction of the long-term creep rupture properties of 9–12%Cr power plant steels. In: Strang A, Conroy RD, Banks WM, Blackler M, Leggett J, McColvin GM, Simpson S, Smith M, Starr F, Vanstone RW, editors. Proceedings 6th Intern Charles Parsons Turbine Conference; 2003; Dublin, Ireland. London (UK): Maney Publishing. p. 427–441.

[12] Lee JS, Armaki HG, Maruyama K, et al. Causes of breakdown of creep strength in 9Cr-1.8W-0.5Mo-VNb steel. Mater Sci Eng A. 2006;428(1–2):270–275. doi: 10.1016/j.msea.2006.05.010

[13] Sawada K, Kushima H, Hara T, et al. Heat-to-heat variation of creep strength and long-term stability of microstructure in Grade 91 steels. Mater Sci Eng A. 2014;597:164–170. doi: 10.1016/j.msea.2013.12.088

[14] Kimura K, Sawada K, Kushima H, et al. Influence of delta ferrite phase on long-term creep strength of

high chromium ferritic creep resistant steels. In: Strang A, Banks WM, McColvin GM, Oakey JE, editors. Proceedings 7th Intern Charles Parsons Turbine Conference; 2007; Glasgow, UK. London (UK): IOM Communications Ltd. p. 465–476.
[15] Sawada K, Sekido K, Kimura K, et al. Effect of initial microstructure on creep strength of ASME Grade T91 steel. ISIJ Int. 2020;60(2):382–391. doi: 10.2355/isijinternational.ISIJINT-2019-358
[16] The Ministry of Economy, Trade and Industry (METI). The interpretation for the technical standard for thermal power plant. 2024:3–4.
[17] American Society of Mechanical Engineers (ASME). ASME boiler and pressure vessel conde. Section II. Part D. Mandatory appendix 1. 2023:1286–1287.
[18] Kimura K, Tabuchi M, Takahashi Y, et al. Long-term creep strength and strength reduction factor for welded joints of ASME grades 91, 92 and 122 type steels. Int J Microstruct Mater Prop. 2011;6(1/2):72–90. doi: 10.1504/IJMMP.2011.040438
[19] Kimura K, Sawada K. History of allowable stresses in Japan and perspective on improvement in creep strength property of grade 91 steel. In: Shingledecker J, Takeyama M, editors. Proceedings Joint EPRI-123HiMAT International Conference on Advances in High Temperature Materials; 2019; Nagasaki, Japan. Ohio (USA): ASM International. p. 47–59. doi: 10.31399/asm.cp.am-epri-2019p0047
[20] American Society of Mechanical Engineers (ASME). ASME boiler and pressure vessel conde. Section II. Part A. 2019.
[21] Japanese Standards Association. Japanese industrial standards (JIS). Method of elevated temperature tensile test for steels and heat-resisting alloys. JIS G. 1998;567:1–13.
[22] Japanese Standards Association. Japanese industrial standards (JIS). Metallic materials – uniaxial creep testing in tension – method of test. JIS Z. 2010;2271:1–48.
[23] Preston-Thomas H. The international temperature scale of 1990 (ITS-90). Metrologia. 1990;27(1):3–10. doi: 10.1088/0026-1394/27/1/002
[24] Larson FR, Miller J. A time-temperature relationship for rupture and creep stresses. Trans ASME. 1952;74(5):765–771. doi: 10.1115/1.4015909
[25] Orr RL, Sherby OD, Dorn JE. Correlations of rupture data for metals at elevated temperatures. NSA-07-006482. NP-4765. Technical Report 27. 1953. doi: 10.2172/4425999
[26] Haque MS, Stewart CM. Metamodeling time-temperature creep parameters. J Press Vessel Technol. 2020;142(3):031504. doi: 10.1115/1.4045887
[27] Kimura K, Kushima H, Abe F. Degradation and assessment of long-term creep strength of high Cr ferritic creep resistant steels. In: Viswanathan R, editor. Proceedings International Conference on Advances in Life Assessment and Optimization of Fossil Power Plants; 2002; Orlando, Florida, USA. Electric Power Research Institute. p. 12-133–12-147.
[28] Kimura K, Sawada K, Kubo K, et al. Influence of stress on degradation and life prediction of high strength ferritic steels. In: Wang YY, editor. Proceedings ASME 2004 PVP Conference; 2004; San Diego, California, USA. New York (USA): ASME. p. PVP2004–2566. doi: 10.1115/PVP2004-2566
[29] Sawada K, Kimura K, Abe F. Mechanical response of 9% Cr heat-resistant martensitic steels to abrupt stress loading at high temperature. Mater Sci Eng A. 2003;358(1–2):52–58. doi: 10.1016/S0921-5093(03)00326-5
[30] Kimura K. Evaluation and extension of allowable stress values for Gr.91. In: Ren W, Nanstad R, editors. Proceedings ASME 2017 PVP Conference; 2017; Waikoloa, Hawaii, USA. New York (USA): ASME. p. PVP2017–65522. doi: 10.1115/PVP2017-65522
[31] American Society of Mechanical Engineers (ASME). ASME boiler and pressure vessel conde. Section III. Division 5. 2019.
[32] Monkman FC, Grant NJ. An empirical relationship between rupture life and minimum creep rate in creep-rupture tests. In: Proceedings ASTM 56; 1956. p. 91-103.
[33] Viswanathan R, Beck CG. Effect of aluminum on the stress rupture properties of Cr-Mo-V steels. Metall Trans A. 1975;6(11):1997–2003. doi: 10.1007/BF03161823
[34] König H, Mayer KH, Keienburg KH, et al. Influence of modern melting techniques on the creep behaviour of heavy-section components of 1% CrMoV steels. Steel Res. 1990;61(6):274–278. doi: 10.1002/srin.199000347
[35] Parker JD, Siefert JA. The creep and fracture behaviour of tempered martensitic steels. Mater High Temp. 2018;35(6):491–503. doi: 10.1080/09603409.2017.1389441
[36] Kimura K, Sawada K, Kushima H. Creep rupture ductility of creep strength enhanced ferritic steels. J Press Vessel Tech. 2012;134(3):031403. doi: 10.1115/1.4005876